Image reconstruction using shift-variant resampling kernel for magnetic resonance imaging

Ahmed S. Fahmy, Bassel S. Tawfik, Yasser M. Kadah*
Biomedical Engineering Department, Cairo University, Giza, Egypt

ABSTRACT

Nonrectilinear k-space trajectories are often used in MRI applications due to their inherent fast acquisition and immunity to motion and flow artifacts. In this work, we develop a more general formulation for the problem of resampling under the same assumptions as previous techniques. The new formulation allows the new technique to overcome the present problems with these techniques while maintaining a reasonable computational complexity. The image space is decomposed into a complete set of orthogonal basis functions. Each function is sampled twice, once with a rectilinear trajectory and the other with a nonrectilinear trajectory resulting in two vectors of samples. The mapping matrix that relates the two sets of vectors is obtained by solving the set of linear equations obtained using the training basis set. In order to reduce the computational burden at the reconstruction time, only a few nonrectilinear samples in the neighborhood of the point of interest are used. The proposed technique is applied to simulated data and the results show a superior performance of the proposed technique in both accuracy and noise resistance and demonstrate the usefulness of the new technique in the clinical practice.

Keywords: Resampling, image reconstruction, magnetic resonance imaging, least-squares problems.

1. INTRODUCTION

In Magnetic Resonance Imaging (MRI), data is collected in the k-space which represents the Fourier transform of the imaged slice. The sampling trajectory along the k-space is determined by the shape of the waveform of the applied magnetic gradients. On-Off gradient waveforms result in evenly spaced k-space samples which can be easily transformed into the image domain using the fast Fourier transform (FFT). Unfortunately, generation of fast switching gradients is not easily accomplished. Thereby smoothly varying gradient waveforms are usually implemented in fast MRI acquisition techniques. However, this results in non-rectilinear sampling trajectories with a multitude of loop-like patterns such as spiral[1,2], radial sampling[2], Rossettes[3], or Lissajous[4]. Such data points must be resampled onto a rectilinear grid in order to take advantage of the speed of the FFT.

Ideal reconstruction is theoretically guaranteed by the sampling theory as long as the Nyquist criterion is satisfied [5,6]. That is, if $f(k)$ is the continuos k-space representation of the imaged slice at a spatial frequency coordinate k, and $S(k- k^r)$ is a sampling function consisting of 2-dimensional evenly spaced impulse functions located at the rectilinear k-space points, k^r, the sampling theory guarantees that $f(k)$ can be completely recovered from its sampled version $f_s(k)= f(k).S(k-k^r)$ as follows[5] ,

$$f(k) = f_s(k)*C(k) \quad , \tag{1}$$

where $C(k)$ is an infinite Sinc function, and * is the convolution operator. Since working with an infinite sinc function is not feasible in practice, truncating the Sinc function is necessary. Substituting $k=k^{nr}$, where k^{nr} is the non-rectilinear k-space grid coordinates and assuming (without loss of generality) that both the rectilinear and the non-rectilinear grids carry the same number of points (=N), then equation (1) can be written in vector form as follows:

$$\boldsymbol{f}^{\mathbf{nr}}{}_{Nx1} = C_{NxN}.\boldsymbol{f}^{\mathbf{r}}{}_{Nx1} \quad , \tag{2}$$

where $\boldsymbol{f}^{r}$, and $\boldsymbol{f}^{nr}$ are vectors containing the rectilinear and the non-rectilinear samples, respectively, while C is a matrix whose entries are $Sinc(k^r-k^{nr})$. In the Uniform Re-Sample algorithm (URS)[4], $\boldsymbol{f}^{r}$ is directly obtained from $\boldsymbol{f}^{nr}$ by inverting

* E-mail: ymk@ieee.org

Medical Imaging 2002: Image Processing, Milan Sonka, J. Michael Fitzpatrick,
Editors, Proceedings of SPIE Vol. 4684 (2002) © 2002 SPIE · 1605-7422/02/$15.00

the matrix C in equation (2). While such matrix inversion can be directly achieved for one-dimensional signals, the URS algorithm becomes impractical in the 2-dimensional signals due to the huge size of the matrix C in this case.

The Block Uniform Re-Sampling algorithm (BURS)[7,8] was introduced by way of approximation to the URS method in order to reduce the computational effort. The BURS algorithm is in essence a numerical method for obtaining the inverse of a large sparse matrix. It is based on isolating a small block, C^{b}_{mxq}, of the matrix C centered at entries (*i*,*j*), where *j* represents an unknown point in $\boldsymbol{f}^{r}$, which is to be estimated from *m* measured non-rectilinear samples centered around the entry *i* in $\boldsymbol{f}^{nr}$. The block is assumed to reasonably approximate the entire mapping (2) for the unknown point *j*. Next, the inverse of the matrix C is obtained, namely C^{b-1}, of which one row corresponding to the sample *j* is kept. This row is used later, during image reconstruction, to estimate the rectilinear sample *j* from the selected few measured samples. This process is repeated for the entire points in $\boldsymbol{f}^{r}$. This method does not guarantee the best available estimate of the resampling process. Moreover, unreasonable estimates of the rectilinear points may be obtained when Lissajous trajectories are used to acquire the k-space as pointed out by Moriguchi, *et al* [4].

In the conventional gridding algorithm[5,6], the measured samples are convolved with a small shift-invariant interpolation kernel, usually a Kaiser-Bessel function, to estimate the rectilinear *k*-space grid. Steps of pre and post compensation of the data are required to reduce certain artifacts inherent to the technique such as cupping or wings[7]. But the main concern in conventional gridding is that the Kaiser-Bessel function is not optimal in the least squares sense, which was shown by Sedarat, et al.[9]. In an attempt to overcome this problem, a methodology was devised to obtain the optimal kernel and showed that it can be shift-variant. However, this method is not readily applicable to high-resolution images because of the associated intensive calculations.

In this paper, we present a new method for estimating of shift-variant resampling kernels that map the non-rectilinear samples to their rectilinear counterparts. Each sample on the rectilinear grid is estimated from its neighboring sampling on the non-rectilinear grid using a least squares criterion. We present the mathematical formulation of the proposed method as well as the results of the implementing the proposed technique compared to those of URS and BURS techniques.

2. THEORY

Estimating a point, *p*, on the rectilinear grid from *m* sampled (non-rectilinear) points can be represented as

$$\boldsymbol{p} = \boldsymbol{a}_{1xm} \cdot \boldsymbol{p}_{mx1} \quad , \tag{3}$$

where $\boldsymbol{p}$ is a vector containing the *m* neighboring samples of the point *p*. For this equation to correctly represent the required mapping from the nonrectilinear grid to the rectilinear one, it should be valid for the k-space of any given image. In other words, if $\Phi=\{\phi_i, i=1{:}L\}$ represents a basis (continuous) functions for the imaged field of view (FOV), then equation (1) should be valid for every ϕ_i. Rewriting (1) for the given set of the basis functions yields the following set of linear overdetermined system of equations,

$$\varphi = \boldsymbol{a} \cdot \boldsymbol{\phi_i} \quad , i=1{:}L \quad , \tag{4}$$

where φ_i is a sample on the rectilinear grid representation of the basis function ϕ_i, and $\boldsymbol{\phi_i}$ is a k-space vector of *m* neighboring samples on the non-rectilinear grid. In vector form, the equations in (2) can be written as

$$\boldsymbol{\varphi}_{1xL} = \boldsymbol{a}_{1xm} \cdot \Phi_{mxL} \quad , \tag{5.a}$$

or,

$$\boldsymbol{a} = \boldsymbol{\varphi} \cdot \Phi^{\dagger} \quad , \tag{5.b}$$

where Φ is a matrix whose columns are the vectors $\boldsymbol{\phi_i}$, and $\Phi^{\dagger}$ is its pseudo-inverse given by $\Phi^{T}.(\Phi.\Phi^{T})^{-1}$. The matrix inverse involved in this pseudo-inverse does not represent a computation burden since $(\Phi.\Phi^{T})$ is an *mxm* matrix (usually *m=9 to 25*). A mapping vector $\boldsymbol{a}$ is calculated for every point on the rectilinear grid. That is, equation (5.b) is solved N^2

times for image size of *N*x*N*. We will call this least-squares resampling based on spatially variant kernel *LR-based* sampling throughout this paper.

3. RESULTS AND DISCUSSION

3.1 One Dimensional Results

The LR-based estimate of the gridding kernel is used to reconstruct 1-dimension signals of finite extent. The functions, ϕ_i, are complex exponentials representing the Fourier transform of spatial domain impulses spanning the entire field of view (fig. 1). In our 1-dimensional simulations, a sampling scheme of the k-space is used such that the sampling density is an integral multiple, referred to as the *density factor* hereon, of the Nyquist sampling rate. The locations of the measured samples, x_i, are given by $x_i=i+r$, where i is a location in the rectilinear grid, and r is a random number such that $|r|<0.5$. The case where the entire set of non-rectilinear samples is used to estimate each rectilinear point ($m=L$) is considered first followed by the case where ($m<<L$).

In the first case ($m=L$), It was found that both the LR-based and the URS techniques give the same results (error below 0.5%), which means that the LR-technique reaches the optimal solution in this case. Interesting results are obtained when the same simulation settings is used but with the sampling trajectory misses one sample. Figures 2.a,b show the reconstruction of the two techniques when the sample at spatial frequency $k=0.7\pi$ is missed (entry 16 in f^{nr}). In Figure 2.a, the signal reconstructed by the LR-based technique overlaps the true signal. At the same time, the URS result suffers artifacts due to the violation of the sampling theorem at certain region in the k-space. These results were obtained without introducing any regularization techniques when obtaining the URS or the LR-based mapping matrices. It was found that truncation of some singular values of the Sinc interpolation matrix used in the URS technique improves the reconstruction yet the LR-based technique is still better (see Figure 2.b). The mapping matrices for both techniques in this case are shown in Figure 3. The effect of varying the location of the missed sample is shown in Figure 4, where the reconstruction error is plotted for both BURS and LR-based algorithms when the location of the missed sample varies from $\pi/16$ to π.

The second case ($m<<L$), is practically a typical case since the target is to reduce the reconstruction time. In the BURS algorithm, the block matrix C^b, of dimension mxq, represents a k-space region of size δkxΔk. This means that m varies from place to another inside the k-space according to the sampling density. In our simulation, m is fixed and the sampling density is made variable. This means that the reconstruction time, which depends on m rather than δk, is fixed allover the k-space regardless what the sampling density is. Moreover, all of the BURS simulations given below use a value of Δk equal ∞ to obtain the best results for BURS.

Table 1 shows the reconstruction error of both the BURS and LR-based techniques at different sampling densities and different values for δk. The reconstruction error of both techniques in the presence of noise is shown in Figure 5.

3.2. Two Dimensional Results

In this section, the LR-based technique is used to reconstruct images acquired using polar trajectories. The images are for numerical phantom and each is of resolution 128*x*128. For each sampling trajectory, a number of sample locations, *m=16*, nearest to each rectilinear point is calculated and stored in a look-up table. The table is used first to construct the required optimal mapping, which is stored also in another table to be used in the resampling process. The number of basis functions used to construct the mapping is taken to be 128^2 thereby, cover the entire FOV with the specified spatial resolution. Calculating the mapping matrix takes about 3.5 hours on a personal computer with PII 400MHz processore and 192 Mbytes of RAM. Image reconstruction takes about 2 seconds on the same workstation (resampling process plus Fourier transformation). Figure 6 shows the LR-based reconstruction in case of polar acquisition of a numerical phantom (Figure 6.b) compared with Fourier reconstruction when rectilinear acquisition is used (Figure 6.a). Cross sectional profiles in the images in Figure 6 are plotted in Figure 7, where we observe that the results from the new method and that of the true almost match each other.

Although the URS algorithm was usually thought of as the perfect resampling algorithm, the results in the previous section indicate that this is not true for all sampling schemes. To demonstrate this, consider the trivial case of resampling data points from a rectilinear grid to the same rectilinear grid. In this case, the samples of the Sinc function used in the URS algorithm, i.e. the rows of the C matrix in (2), will take unity value at one location corresponding to the

row index and zeros in the rest. Therefore, C is an identity matrix of size *NxN*. If one sample is missing from the measurements, the corresponding column in the C matrix is also missed turning the problem into an underdetermined system of equations. Therefore, the obtained solution is the minimum norm solution, and in the above case the missing sample will be substituted for by zero. On the other hand, the proposed method still provides the least squares solution for the same problem. That is, when the mapping is being established by equation (5), the problem is still over-determined because the basis vectors outnumber the grid points, i.e. the number of columns in matrix Φ is larger than the number of rows. This conclusion can also be illustrated by examining the mapping matrices in Figure 3, where the mapping matrices are shown to be band-limited in general. Nonetheless, when a sample is missing, the URS matrix ignores its absence while the proposed method matrix tries to estimate it based on the larger set of the non-rectilinear samples. Moreover, regularization techniques should be used for the URS algorithm to give acceptable reconstruction results. It was found that the regularization depends on the location where the sample is missing and since many samples are expected to be missing in practical situations, it might be difficult to achieve reasonable regularization.

As mentioned earlier, the main concern in any resampling or gridding algorithm is to reach optimal reconstruction meanwhile maintain the reconstruction time at low limit. The proposed method in this work establishes a mapping between each rectilinear point and a given finite number of neighboring points on the non-rectilinear grid. For each rectilinear point, the mapping is not restricted to certain functional form, instead, it is determined through an optimization process based on a least squares error criterion. Consequently, the obtained mapping is shift-variant which is apparent clearly in Figure 3. This result contradicts with the thoughts involved in the current resampling algorithms, which rely mainly on the convolution with a shift-invariant kernel (e.g., Sinc, Kaiser-Bessel, etc.). However, a work of Sedarat et al.[9] showed that the optimal mapping can be shift-variant but the methodology used to obtain such mapping requires intensive computations and thus not readily applicable to high-resolution images. Moreover, although our simulations show that the mapping is complex, we can observe that the reconstruction error when ignoring the imaginary part is almost the same. This approximately halves the computational time of the resampling process and reduces the memory size required for storing the mapping matrix.

From Table 1, it is obvious that the reconstruction error of the LR-based technique is lower than that of the BURS technique especially at small values of δk (the smaller the values of δk, the lower the reconstruction time and memory requirements). At large values of δk, e.g. 2.5, the performance of both techniques is nearly the same. Unexpectedly, there is a rise in the reconstruction error at δk =1.5 this is because this result is given by using only three non-rectilinear samples to estimate each rectilinear point.

Finally, although the described LR-based algorithm is applied to resample the data from a non-rectilinear grid to rectilinear one, it can be used to establish mapping between arbitrary grids by changing the locations of the samples in the two vectors f^{r}, and f^{nr} in equation (2). The proposed LR-algorithm achieves the required mapping on one step only. This is faster than the method proposed by Rasche et al.[10], which requires a two-step convolution interpolation.

4. CONCLUSIONS

In this work, a least squares error solution is developed to resample data points from a non-rectilinear grid into a rectilinear grid. The results of this work show that the URS algorithm is not the optimal method in the least squares sense when the sampling density decreases below the Nyquist limit. The proposed technique, on the other hand, is superior in the least squares sense regardless of the sampling pattern. Moreover, the proposed algorithm does not restrict the mapping to be shift-invariant or real valued which allows more freedom to achieve optimality. Future work includes the potential of the new method to be extended for use in extrapolation besides interpolation or resampling.

REFERENCES

1. E. Haacke, R. W. Brown, M. R. Thompson, and R. Venkatesan, *Magnetic Resonance Imaging: Physical Principles and Sequence Design,* John Wiley & Sons, New York, 1999.
2. C. H. Meyer, B. S. Hu, D. G. Nishimura, and A. Macovski, "Fast spiral coronary artery imaging," *Magnetic Resonance in Medicine,* vol. 28, pp 202-213, 1992.
3. D. C. Noll, S. J. Peltier, and F. E. Boada, "Simultaneous Multislice Acquisition Using Rosette Trajectories (SMART): A New Imaging Method for Functional MRI," *Magnetic Resonance in Medicine,* vol. 39, pp. 709-716, 1998.

4. H. Moriguchi, M. Wendt, and J. L. Duerk, "Applying the Uniform Resampling (URS) algorithm to Lissajous trajectory: Fast image reconstruction with optimal gridding," *Magnetic Resonance in Medicine*, vol. 44, pp 766-781, 2000.
5. J. I. Jackson, C. H. Meyer, D. G. Nishimura, and A. Macovski, "Selection of a convolution function for Fourier inversion using gridding," *IEEE Trans. Medical Imaging*, vol. 10, no.3, pp. 473-478, Sept. 1991.
6. J. D. O'Sullivan, "A fast sinc function gridding algorithm for Fourier inversion in computer tomography," *IEEE Trans. Medical Imaging*, vol. 4, no. 4, pp. 200-207, 1985.
7. D. Rosenfeld, "An optimal and efficient new gridding algorithm using singular value decomposition," *Magnetic Resonance in Medicine*, vol. 40, pp 14-23, 1998.
8. H. Moriguchi, and J. L. Duerk, "A modified block uniform resampling (BURS) algorithm using truncated singular value decomposition: fast gridding with noise reduction," *Proc. International Society of Magnetic Resonance in Medicine*, Glasgow, 2001.
9. H. Sedrat, and D. G. Nishimura, "On the optimality of the gridding reconstruction algorithm," *IEEE Trans. Medical Imaging*, vol. 19, no.4, pp. 306-317, April 2000.
10. V. Rasche, R. Proska, R. Sinkus, P. Bornert, and H. Eggers, "Resampling of data between arbitrary grids using convolution interpolation, *IEEE Trans. Medical Imaging*, vol. 18, no. 5, pp. 385-392, May 1999.

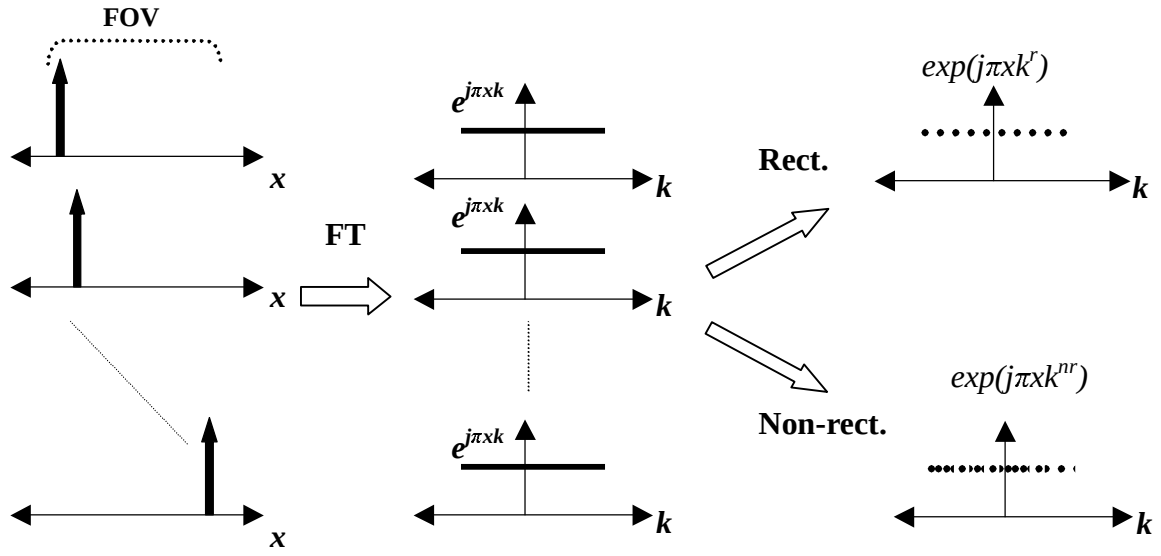

Figure 1. The basis set used in the LR equations are the Fourier transforms of impulse functions spanning the field of view. Note that the magnitude of the functions φ_i are the same and equal to unity while the phase (not shown) depends on the location of each impulse, *x*.

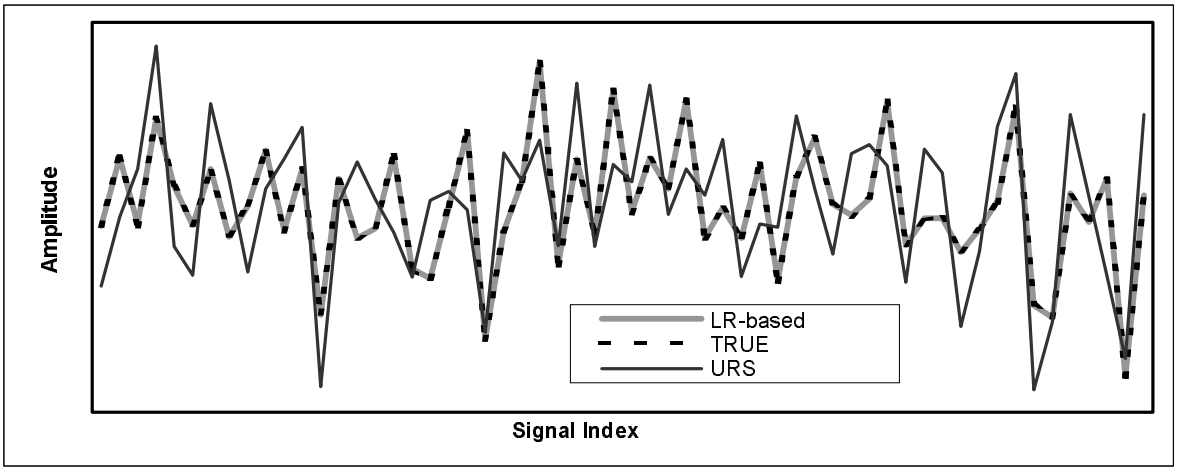

Figure 2.a Reconstruction using URS versus LR-based technique, both are without regularization.

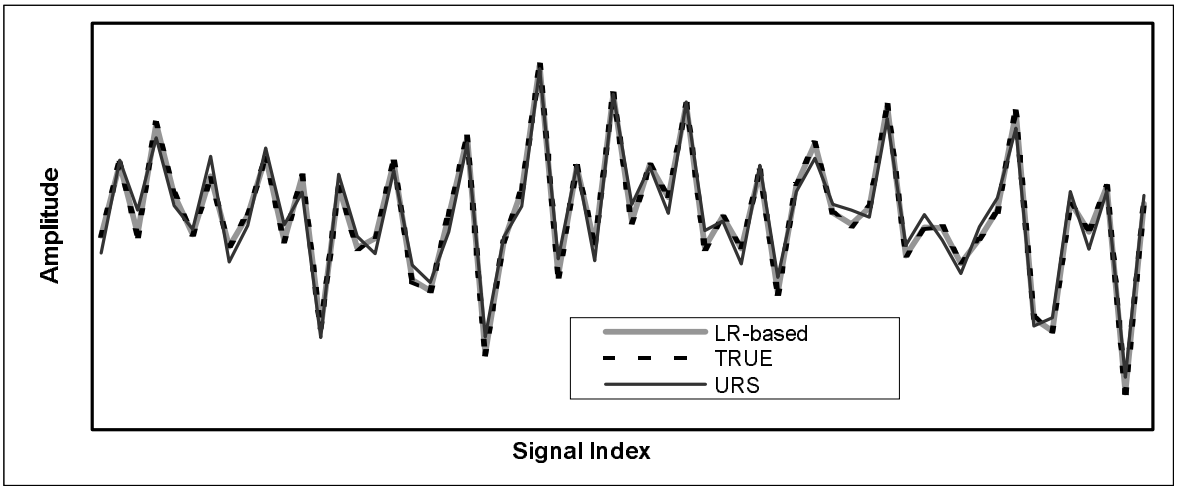

Figure 2.b Reconstruction using URS (with regularization) versus LR-based technique.

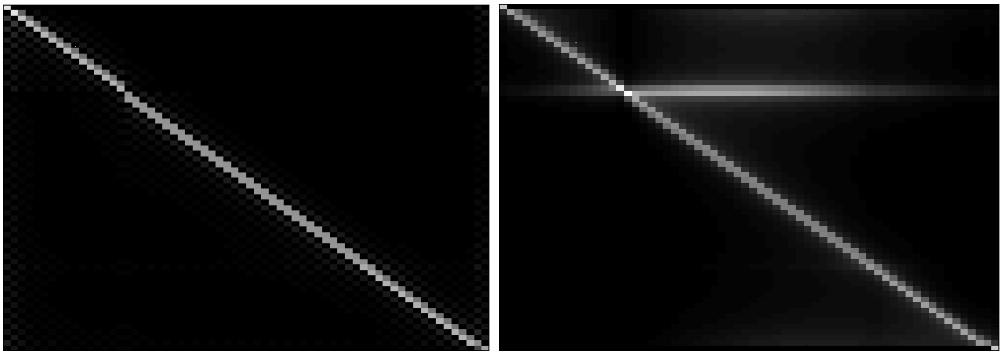

Figure 3. The mapping matrix of the URS (left) and LR-based technique (right). Note the difference at row number 16, where the trajectory has missed a k-space sample.

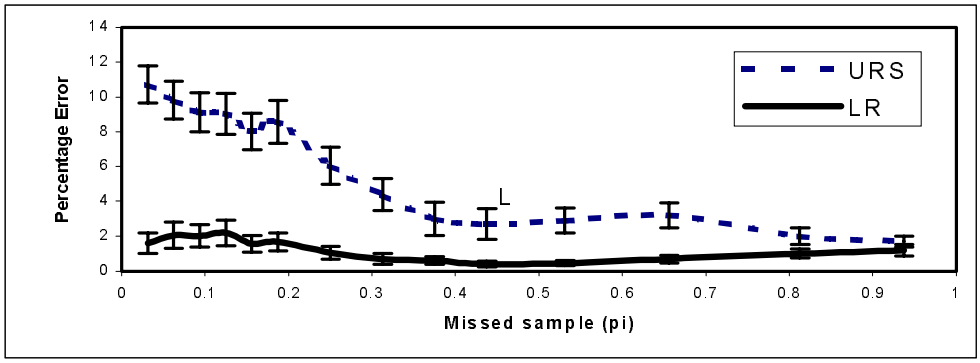

Figure 4. Reconstruction error using URS and LR-based algorithms when the missed sample varies from $\pi/16$ to π.

Density Factor	8	8	10	8	6	4	2	8	2
# Points, *m*	5	7	11	9	7	5	3	13	5
Corresponding δk	***.625***	***.875***	***1.1***	***1.125***	***1.167***	***1.25***	***1.5***	***1.625***	***2.5***
LR-***based***	3.5%	3%	0.6%	.56%	.47%	0.78%	9.5%	0.23%	0.6%
BURS (Δk=∞)	17.5%	14.1 %	11.9%	11.8%	9.7%	3.3%	10.2%	2%	0.8%

Table 1. Reconstruction error of both LR-based and BURS techniques at different sampling densities and different values for *m*.

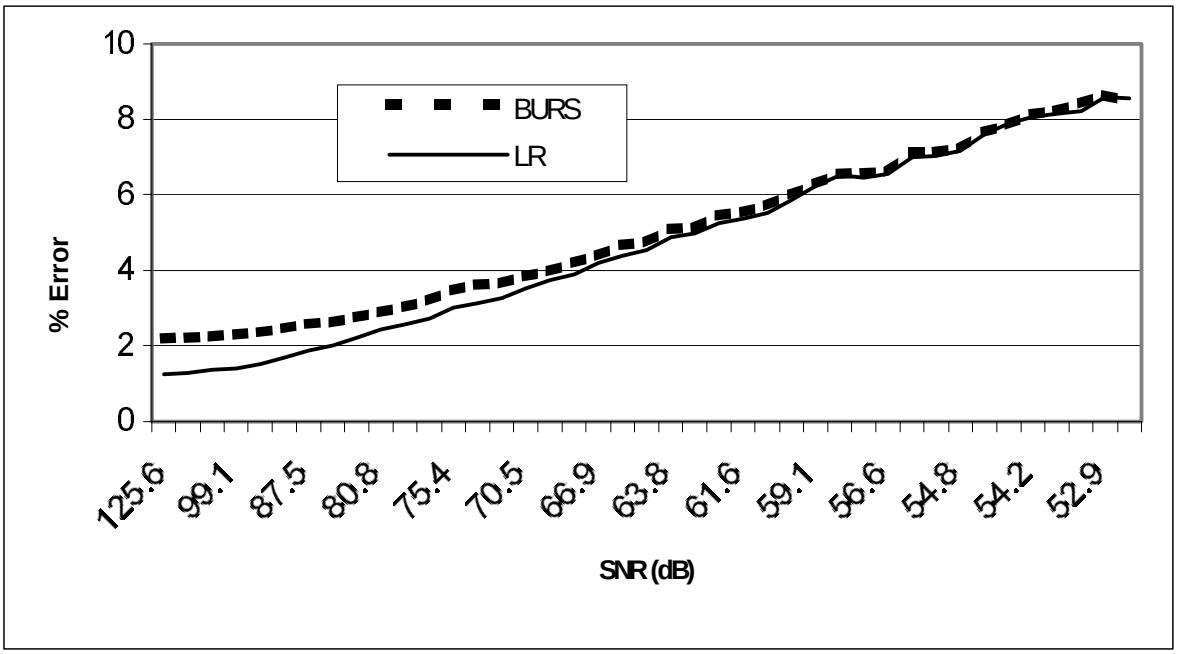

Figure 5. Reconstruction error using URS and LR-based algorithms in presence of noise.

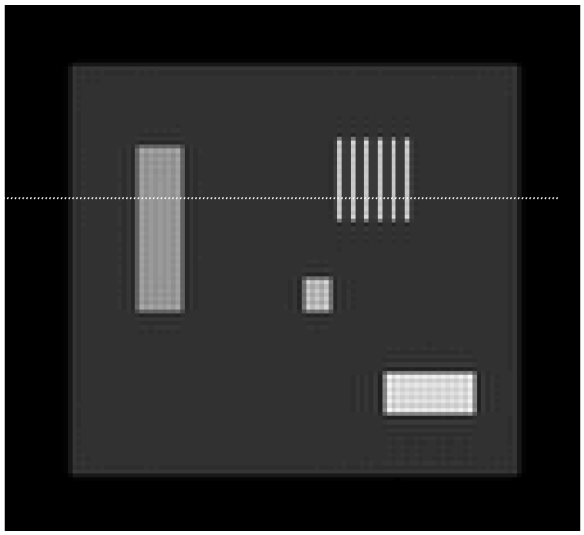

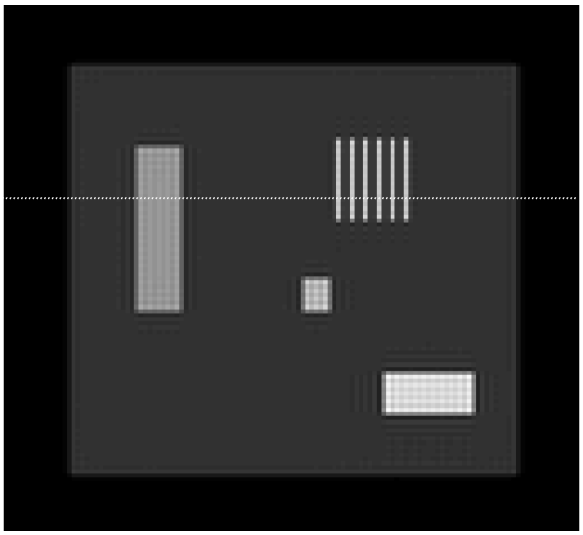

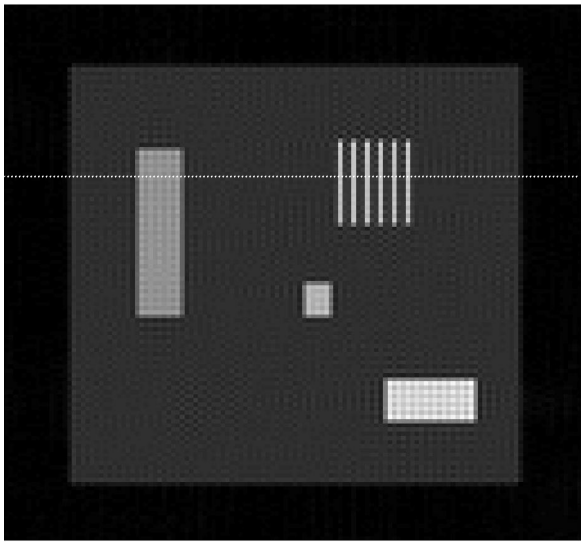

Figure 6. Phantom image when acquired using rectilinear trajectory (a), and when acquired using polar trajectories and reconstructed using LR-based and BURS algorithms in (b), and (c) respectively.

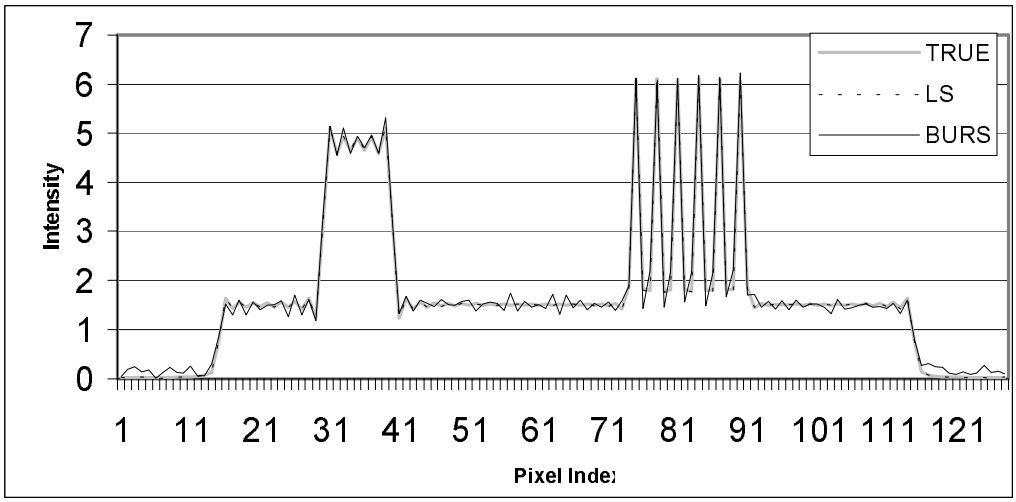

Figure 7. Cross-sectional profiles of the images in Figure 6 at the level of the dotted white line. It is shown that the LR-based reconstructed image coincides with the true one.